Quantitative Fundus Autofluorescence in Healthy Eyes

Jonathan P. Greenberg,[1] Tobias Duncker,[1] Russell L. Woods,[2] R. Theodore Smith,[1,3] Janet R. Sparrow,[1] and François C. Delori[2]

[1]Department of Ophthalmology, Harkness Eye Institute, Columbia University, New York, New York
[2]Schepens Eye Research Institute and Department of Ophthalmology, Harvard Medical School, Boston, Massachusetts
[3]Department of Ophthalmology, New York University, New York, New York

Correspondence: François C. Delori, Schepens Eye Research Institute, 20 Staniford Street, Boston, MA 02114; francois_delori@meei.harvard.edu.

Submitted: May 20, 2013
Accepted: July 8, 2013

Citation: Greenberg JP, Duncker T, Woods RL, Smith RT, Sparrow JR, Delori FC. Quantitative fundus autofluorescence in healthy eyes. *Invest Ophthalmol Vis Sci.* 2013;54:5684–5693. DOI:10.1167/iovs.13-12445

Purpose. Fundus autofluorescence was quantified (qAF) in subjects with healthy retinae using a standardized approach. The objective was to establish normative data and identify factors that influence the accumulation of RPE lipofuscin and/or modulate the observed AF signal in fundus images.

Methods. AF images were acquired from 277 healthy subjects (age range: 5–60 years) by employing a Spectralis confocal scanning laser ophthalmoscope (cSLO; 488-nm excitation; 30°) equipped with an internal fluorescent reference. For each image, mean gray level was calculated as the average of eight preset regions, and was calibrated to the reference, zero-laser light, magnification, and optical media density from normative data on lens transmission spectra. Relationships between qAF and age, sex, race/ethnicity, eye color, refraction/axial length, and smoking status were evaluated as was measurement repeatability and the qAF spatial distribution.

Results. qAF levels exhibited a significant increase with age. qAF increased with increasing eccentricity up to 10° to 15° from the fovea and was highest superotemporally. qAF values were significantly greater in females, and, compared with Hispanics, qAF was significantly higher in whites and lower in blacks and Asians. No associations with axial length and smoking were observed. For two operators, between-session repeatability was ±9% and ±12%. Agreement between the operators was ±13%.

Conclusions. Normative qAF data are a reference tool essential to the interpretation of qAF measurements in ocular disease.

Keywords: lipofuscin, melanin, quantitative fundus autofluorescence, retina, retinal pigment epithelium, scanning laser ophthalmoscope

The retina exhibits an inherent autofluorescence (AF) that originates principally from lipofuscin fluorophores in RPE cells.[1] The known lipofuscin pigments constitute a complex mixture of bisretinoids[2–6] that originate in photoreceptor cells and are deposited secondarily in the RPE as components of phagocytosed outer segment membrane. Peak excitation of the known bisretinoids range between approximately 430 and 510 nm,[3–6] and could account for the excitation spectrum of AF observed in vivo.[1]

Lipofuscin has been studied by fluorescence and morphometric analyses and efforts were made to quantify it.[7–10] The age dependency of lipofuscin accumulation was established from fluorescence intensities in histologic sections with confirmation by morphometric analysis and peripheral versus central differences in concentration were ascertained. Subsequently, fundus AF was characterized in in vivo studies using a fundus fluorophotometer[11] designed to measure excitation and emission spectra from small retinal areas.[1] Images of fundus AF were also acquired by modified fundus cameras[12,13] and by an adaptive optics system.[14] For 2 decades however, the most customary approach has been to image fundus AF by confocal scanning laser ophthalmoscopy (cSLO)[15–17] and the routine clinical use of this device has grown.[18] Fundus AF profiles constructed from gray scale intensity values obtained along a horizontal axis centered over the fovea,[19] roughly confirmed the topographic distribution mapped photometrically.[20] In addition, cSLO images of AF intensity mapped to a color scale and horizontal and vertical profiles of AF intensity have shown that the intensities can vary in the presence of recessive Stargardt disease.[21] Other retinal diseases exhibiting discordant patterns of fundus AF include Best macular dystrophy, retinitis pigmentosa, AMD, and acute macular disease.[21–29]

Despite the wide-spread use and clinical utility of fundus AF, attempts to reliably measure and compare AF intensities in fundus images have met with difficulty. Recently, however, a standardized clinically accessible approach to the objective quantitation of fundus AF intensities (qAF) in human subjects was described. The method incorporates a standard fluorescent reference into the imaging device.[30] The reference compensates for changes in laser power and detector gain and allows comparison of images obtained longitudinally or using devices at different sites.

Here, we have gathered normative data for qAF from a large number of healthy participants aged 5 to 60 years. The objective of the study was to establish the range and distribution of qAF values with respect to age, sex, race/ethnicity, and smoking status. This aim necessitated the implementation of strict image acquisition and analysis protocols. These normative data from a large nonclinical population sample were collected to both describe and to

Table 1. Study Population

Groups	Number of Subjects/Eyes	Ages		Females/Males	Refractive Error		Smoking Status: Current/Ever‡	Brown Iris
		Mean, y	Range, y		Mean, D	Range, D		
Whites	87/125	31.8	6–58	43/44	−1.0	−9 to 6	7/21	28
Hispanics*	79/107	30.1	5–60	46/33	−0.9	−8 to 6	8/15	78
Blacks	47/57	36.6	9–56	23/24	−1.2	−9 to 3	4/6	47
Asians	43/56	36.5	22–59	25/18	−3.0	−9 to 2	4/10	43
Indians	6/9	32.1	25–39	4/2	−2.5	−5 to 0	0/1	6
Other and mixed†	15/20	27.5	10–57	9/6	−0.7	−6 to 4	1/4	14
All	**277/374**	**32.6**	**5–60**	**150/127**			**24/57**	**216**
% of all subjects	100%			54/46%			9/21%	78%

Bold indicates the sum of values for all race/ethnicity groups.

* These were subjects originating from Latin America who were not otherwise classified as another race.

† These were six subjects (10 eyes) reporting more than one race, seven subjects (8 eyes) reporting one race and Hispanic, and two subjects (2 eyes) reporting another race (not white, black, Asian, or Indian).

‡ The "ever" category includes the current smokers (i.e., current plus previous).

understand the variables inherent in fundus AF. Going forward, these normal values will allow us to view a particular value in context rather than in isolation so that we can assess whether a given clinical value might be considered typical.

Methods

Study Population

The study population consisted of 277 subjects (374 eyes) with healthy ocular status aged 5 to 60 years (Table 1). Subjects had no visual complaints, no family history of inherited retinal disease, no history of ocular disease or eye trauma, no systemic disease that may affect the retina other than controlled hypertension, and had not taken medications known to affect the retina or ocular media, such as chloroquine, hydroxychloroquine, vigabatrin, or chlorpromazine.

Refraction and corneal curvature were determined using the Auto Ref/Keratometer ARK-530A (Nidek Co. Ltd., Gamagori, Japan). Axial length was also measured in 65% of the eyes using the Zeiss IOLMaster (Carl Zeiss, Jena, Germany). Subjects had clear media except for occasional floaters. However, for some subjects over 45 years of age, slit-lamp examination revealed traces of nuclear sclerosis.

To characterize ocular (stromal) melanin pigmentation, iris color was self-reported and confirmed by examination, as brown or not brown (blue, green, and hazel). Smokers were defined as those subjects reporting having ever smoked and those that were current smokers. Pack years were determined from subject reports.

The tenets of the Declaration of Helsinki were followed, institutional review board approval was granted from Columbia University, and informed consent was obtained for each subject. The pupil of the test eye was dilated to at least 6.5 mm in diameter using 1% tropicamide and 2.5% phenylephrine. The retinal light exposures (beam power: 280 μW; 488 nm, 30° × 30° field) were below the limits recommended by the American National Standards Institute for durations longer than 8 hours. For a typical measurement session in this study (duration: 30 seconds), the retinal irradiance was 450 times below the maximum permissible exposure.[31,32]

Image Acquisition

Two experienced operators (JPG, TD) acquired AF images using a Spectralis HRA+OCT (S3300; Heidelberg Engineering, Heidelberg, Germany), modified by insertion of an internal fluorescence reference to correct for variable laser power and detector sensitivity.[30] Excitation was 488 nm and the barrier filter transmitted light from 500 to 680 nm. All AF images were recorded for a 30° × 30° field (768 × 768 pixels) in the high-speed mode (8.9 frames/s) as a mean of 9 frames.

Room lights were turned off and the subject's head was positioned in the chin–head rest. The camera was aligned to the eye under near-infrared (NIR) illumination, good focus was attained, and an NIR image was recorded. The camera was then retracted, AF mode was enabled, and it was slowly moved forward, allowing the patient to adjust to the excitation light. It was aligned in all three dimensions to obtain an image with maximum uniformity, and care was taken to precisely locate the beam in the center of the pupil. The fundus image was focused to reach maximum AF signal intensity, and the detector sensitivity was adjusted to avoid nonlinear effects. This period of adjustment in the AF mode must last at least 20 seconds as it also serves as a bleaching exposure to reduce AF attenuation by rod photopigment to less than 2%.[30] Before the acquisition of each image, the patient was asked to blink to provide a uniform tear film on the cornea. Eyelid interference was avoided, sometimes with the help of an assistant. At least three images (each of 9 frames, acquired in video format) were obtained, often with minor camera realignment between each acquisition. The quality of subject fixation (excellent/good/average/poor) was recorded, along with any subject related difficulties, such as floaters, photophobia, and dry eyes.

To assess reproducibility, a second imaging session was performed a few minutes after the first session in 233 eyes. Between the two sessions the subject sat back and the camera position and focus were randomly changed. Thus, the second session required repositioning of the subject and realignment and focusing. Both operators performed imaging in 38 eyes to assess interoperator agreement. Finally, interocular agreement was assessed in 97 subjects (the right eye was measured first in 75% of these comparisons).

Image Analysis

Frames of each image (video) were examined and two satisfactory images, based on consistent signal intensity, were selected from each session. The frames of these videos were aligned and averaged with the system software and saved in the nonnormalized mode (no histogram stretching) to create the images for analysis. If two suitable 9-frame images were not available, those demonstrating either localized (eyelid interference) or generalized (iris obstruction) decreased signal were eliminated before averaging (necessary in ≈10% of images, never less than four acceptable frames). Two experienced

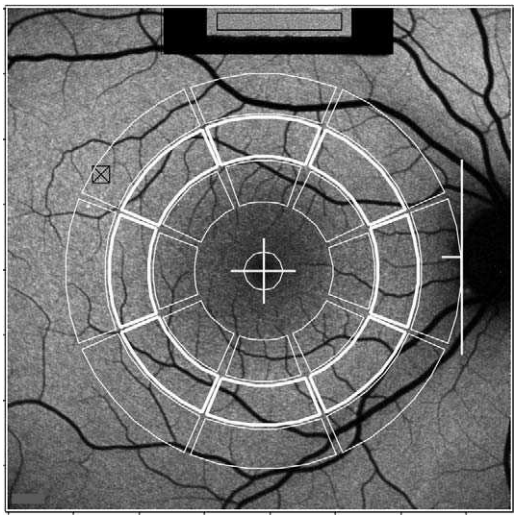

FIGURE 1. qAF by image analysis. Measurement areas (outlined in *white*) consist of three concentric rings (outer, middle, and inner) divided into eight segments, and a circular foveal area. Values used in the current work were obtained in the middle ring marked by thickened lines. The positions of the segments are all dependent upon the horizontal distance *FD* between the fovea (+) and the temporal edge of the disc (*white line*). The radii of the centerlines expressed in pixels (or in degrees visual angle, for the average value of $FD = 315$ pixels), for the outer, middle, and inner, are $0.90 \times FD$ (11.1°), $0.68 \times FD$ (8.4°), and $0.46 \times FD$ (5.7°), respectively. The thickness of the segments is $0.2 \times FD$ pixels (2.5°) and the angles subtended by the segments are 40°. The central circle (fovea) has a radius of $0.1 \times FD$ pixels (1.2°). The internal fluorescent reference (*top*) was recorded simultaneously with the image; the GL_R was measured in the rectangular area outlined in *black*. The area of highest AF in the image is indicated by a *square* and *cross*.

operators (JPG, TD) agreed on which images should be selected and whether any frames should be rejected.

AF images were analyzed with a dedicated image analysis program (IGOR; WaveMetrics, Inc., Lake Oswego, OR). The program identified the temporal edge of the optic disc and the position of the fovea, with adjustment by the operator in some cases. When a myopic crescent (low AF) obscured the anatomical edge of the disc, an NIR image (crescent has high reflectance) aided identification of the disc edge. The horizontal distance between the edge of the disc and the foveal center (FD) was used to define the measurement areas that consisted of eight segments organized in three concentric rings around the fovea as well as a circular foveal area (Fig. 1). Segments extending further than 15° from the center of the image (due to off-center location of the fovea) were eliminated.

As described previously,[30] to derive qAF, we combined the mean gray level of each segment (GL_S) with the GL_R measured at the internal reference, and the GL_0 corresponding to zero-laser light, using:

$$qAF = RCF \times \frac{GL_S - GL_0}{GL_R - GL_0} \times \left[\frac{SF}{SF_{em,7.7}}\right]^2 \times \frac{T_{media,20}}{T_{media,age}} \quad (1)$$

The reference calibration factor (RCF) was obtained for the internal reference of the device by calibration with an external fluorescent "master reference." The scaling factor (SF, in retinal micrometers/pixel) accounted for magnification differences between subjects; SF was calculated from the focus setting of the Spectralis and the corneal curvature of the subject and was referenced to the SF of an emmetropic eye (7.7-mm corneal curvature). For the transmission of the ocular media, we used normative data for the media transmission at a given age and wavelength[33] ($T_{media,age}$, combined for excitation and emission wavelengths) and the $T_{media,20}$ of a 20-year-old subject for normalization. The media correction term was:

$$\frac{T_{media,20}}{T_{media,age}} = 10^{5.56 \times 10^{-5} \times (age^2 - 400)} \quad (2)$$

The factor $T_{media,20}/T_{media,age}$ gradually increases from 0.95 at age = 5, to 1.00 at age = 20, and to 1.51 at age = 60 years.

Thus, qAF reflects fundus AF relative to that which would be measured through the media of a 20-year-old emmetropic eye with average ocular dimensions.

Data Analysis and Statistics

For each image, we calculated the mean qAF_8 of the eight segments in the middle ring (Fig. 1) to average the anatomical spatial distribution and minimize the instrumental nonuniformities. For the full model, in each eye we averaged all qAF_8 obtained in one or two sessions, or by one or two operators. Individual qAF data from all segments in all rings were used to assess the spatial distribution of the AF.

To investigate the effects on qAF of age, sex, race, ocular pigmentation, refraction (spherical equivalent), axial length, and smoking status, we used mixed-effects linear regression that accounts for within-subject correlations between eyes (Stata, College Station, TX). After trying various models, the best linear fit was obtained with an exponential model of the form:

$$\log(qAF_8) = B_0 + B_1 factor_1 + \ldots + B_n factor_n + B_{age}\log(age) \quad (3)$$

this can be rewritten as:

$$qAF_8 = 10^{(B_0 + B_1\, factor_1 + \ldots + B_n\, factor_n)} \cdot age^{B_{age}} \quad (4)$$

where $factor_1$ to $factor_n$ were a combination of binary and continuous factors. The binary factors in the model included sex, race/ethnicity (e.g., reporting Asian heritage, yes or no), smoking status, and iris color (brown or not brown). Continuous factors included pupil diameter in millimeters and other acquisition-specific parameters. The final model was developed by entering factors and then progressively removing nonsignificant factors ($P > 0.15$). Age was included in all models as it was the main predictive factor. Fifteen subjects had no unique race/ethnicity (Table 1). Models that included race/ethnicity were developed both by including only the 262 participants with a unique race/ethnicity (354 eyes) and by including all 277 subjects (374 eyes). Those models were not substantively different.

To evaluate the repeatability of the measurement between sessions and the agreement between the two operators we used the method of Bland-Altman[34] for the differences ($\log[qAF_2] - \log[qAF_1]$), where qAF_1 and qAF_2 were the two measures under consideration. For the population considered here and for a previous study[20] the variance in qAF was found to increase with age. However, the variance in log(qAF) does not change with age, allowing for an estimation of the measurement variability for all ages.

RESULTS

Spatial Distribution

Determination of the spatial distribution of lipofuscin from AF images is inevitably affected by instrumental nonuniformities in

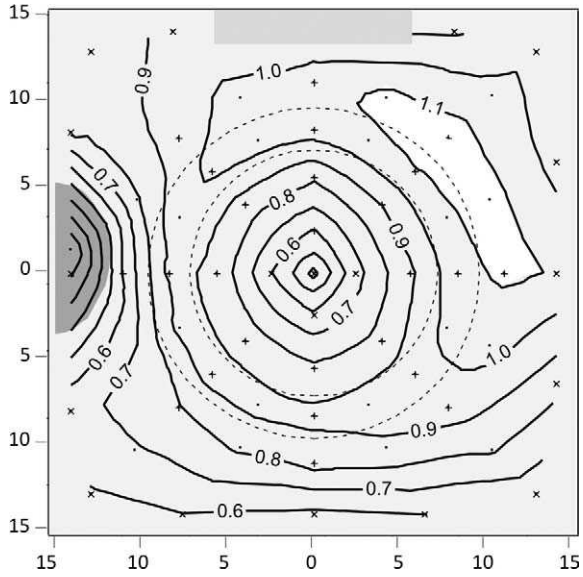

FIGURE 2. Contour plots describing the average distribution of the AF obtained from the 97 subjects with data for both eyes. The data is presented as a left eye. The axes indicate the retinal eccentricity in degrees relative to the center of the fovea. The numbers for each contour are relative qAF (qAF_i/qAF_8) where qAF_8 is the mean of the eight segments of the middle ring delineated by the two concentric interrupted *black lines*. The sampling areas were the 24 segments (+ *sign*; areas: 6600–12,400 pixels^2) and additional locations (*X sign*; areas: 2000–10,000 pixels^2) near the center and at the edges and corners of the image. *Single dots* are locations where linear or quadratic interpolations were used. The coefficients of variation for these relative data were 4% to 6% for the middle ring, 4% to 9% for the inner and outer rings (except near the optic disc: 9%–14%), and 15% to 25% inside the inner ring reflecting the variability in amount and extent of RPE melanin and of macular pigment. The *gray rectangle* marks the position of the internal fluorescent reference.

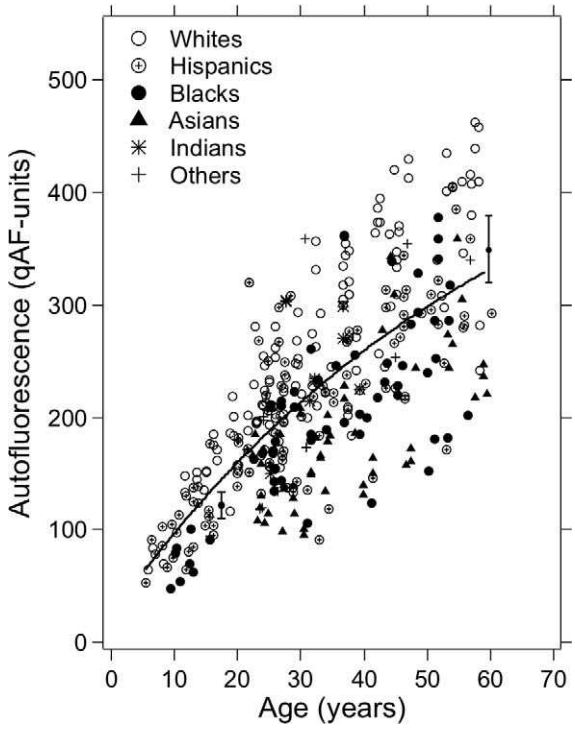

FIGURE 3. qAF in 277 subjects (aged 5–60 years) with healthy retinal status. Mean qAF_8 intensity units, obtained by averaging the eight segments in the middle ring shown in Figure 1, are plotted as a function of age and subjects are grouped according to race/ethnicity. The *solid curve* is an exponential fit to the full sample (374 eyes). The two *brackets* at the arbitrary qAF values (125 and 350 qAF-units) illustrate the ±95% confidence limits (twice the SD) corresponding to the measurement variability (±9.4% of qAF).

laser power and/or detection efficiency across the image field. Tests on uniform fluorescent patterns (Supplementary Data S1) revealed a decrease in signal with increasing eccentricity from the center of the image; at an eccentricity of approximately 10°, this decrease was approximately 10%. Additionally, at the eccentricity of the middle ring there were asymmetries, with the right and top sides of the image being 3% to 4% higher than the left and the bottom sides, respectively. This asymmetry was slightly greater vertically.

Qualitatively similar instrumental asymmetries were detected in fundus AF images (Supplementary Data S2) by comparing left and right eyes (97 subjects) since it can be assumed that the distribution of lipofuscin is the same in both eyes. We found a horizontal asymmetry with the right side of the image being approximately 6% higher than the left (middle ring). We assessed vertical asymmetries by comparing (6 eyes, 3 subjects) images acquired with the head tilted clockwise and counterclockwise by 80° to 90°. A vertical asymmetry was found with the top of the image being approximately 8% higher than the bottom of the image. Both horizontal and vertical asymmetries increased with greater eccentricity from the center of the image.

Despite these nonuniformities, we estimated the spatial distribution of qAF, by averaging normalized qAF's (qAF_i/qAF_8) from the left and right eye (respecting the mirror symmetry) thereby correcting for the horizontal asymmetries (Fig. 2). This relative spatial distribution does not account for the drop in signal toward the edges of the image or for the vertical instrument asymmetries. The maximum relative qAF in the superotemporal quadrant could be overestimated by an average of 4% due to the vertical asymmetries detected in the three subjects (assuming asymmetries varied monotonically across the field).

For all assessments in this study, we utilized the qAF in the eight segments of the middle ring to calculate mean qAF_8 (Fig. 1); this approach minimized the effects of instrumental nonuniformities and provided a single value for analyses. Each of these values is representative of the entire image (outside the central area occupied by macular pigment) since the qAF values for segments in the middle ring were highly correlated with each other ($r > 0.96$, $P < 0.0001$) as were the average qAF in each of the three rings of segments ($r > 0.96$).

Effects of Age and Other Factors

The relationship between qAF_8 and age for the different race/ethnicity groups is shown in Figure 3. The full model that was developed from the mixed-effects linear regression for our sample was (incorporating only terms that were $P \leq 0.15$):

$$\begin{aligned}\log(qAF_8) = {} & 1.097 + 0.730 \cdot \log(age) - 0.31 \cdot male + 0.0075 \\ & \cdot right\text{-}eye + 0.084 \cdot white - 0.043 \cdot black \\ & - 0.086 \cdot asian + 0.023 \cdot eversmoker + 0.016 \\ & \cdot pupil\text{-}diameter - 0.013 \cdot defocus\end{aligned} \quad (5)$$

where the terms male, right-eye, white, black, Asian, and ever smoker were binary indicating presence or absence of that feature. The terms age, pupil-diameter, and defocus were continuous variables in units of years, millimeters, and diopters (D), respectively. The factor defocus was the difference

Table 2. Coefficient *B* for the Mean and for the 95% Confidence Limits for People Only Reporting One Race/Ethnicity

Race/Ethnicity Groups	Coefficients		
	B for Mean	Lower 95% CL	Upper 95% CL
Whites*	19.98	14.29	27.95
Hispanics*	16.64	10.14	27.31
Blacks*	14.48	8.56	24.47
Asians*	13.11	8.24	20.86
Indians*	18.31	11.86	26.28
All subjects†	19.08	11.07	32.88

* The qAF is calculated as $qAF = \mathrm{B} \cdot age^{0.732}$, where the power 0.732 is used for all groups. The 95% confidence limits (CL) are (lower 95% CL) $\cdot\ age^{0.732}$ and (upper 95% CL) $\cdot\ age^{0.732}$. All resulting predictions are in qAF-units.

† For all subjects with defined race/ethnicity. Between-subject variability in log(qAF) is ±(log[32.88] − log[19.08]) or ±0.24 log qAF-units. Between-subject variability in qAF is 0.5 (32.88–11.07)/19.08 or ±57% of the mean qAF. The age relationship is described by $age^{0.691}$.

between the refractive error corresponding to the focus of the Spectralis and that measured using the autorefractor.

The strongest effect was an increase in qAF_8 with age ($P < 0.001$). Race/ethnicity was also an important factor. Considering only subjects with a unique race ($n = 257$), whites had the highest qAF_8, higher than all other races ($P < 0.001$) except Indians ($P = 0.44$). Indians had higher qAF_8 than blacks ($P = 0.02$) or Asians ($P = 0.001$), but not significantly more than Hispanics ($P = 0.26$). Hispanics had higher qAF_8 than blacks ($P = 0.006$) or Asians ($P < 0.001$), and blacks had higher qAF_8 than Asians ($P = 0.03$).

On average, qAF_8 was slightly higher (by 1.7%, $10^{0.0075} = 1.017$) in the right than the left eye ($P = 0.01$) and was lower (by 7.4%) in males as compared with females ($P = 0.01$). qAF_8 increased slightly with increasing pupil size ($P = 0.02$) and decreased with increasing defocus ($P = 0.01$). There was a tendency for qAF_8 to increase in those who had ever smoked ($P = 0.14$), but being a current smoker or number of pack years were not associated with qAF_8 ($P > 0.30$). Males were less likely to be current smokers than females ($\chi^2 = 0.58$, $P = 0.02$), but the interaction term male smoker was not significant ($P = 0.13$). Axial length was not associated with qAF_8 ($P = 0.18$). Fixation quality was correlated with qAF_8 ($r = -0.25$, $P < 0.001$), but was not associated with qAF_8 when corrected for age ($P = 0.62$). Younger subjects had worse fixation quality (Spearman $r = -0.23$, $P < 0.001$).

Simplified Model and Confidence Limits

To provide a normative model for clinical studies, we removed the factors that produced small effects (sex, eye, pupil diameter, ever smoker, and defocus), and also included only the 262 subjects (354 eyes) reporting a single race or ethnicity (removing the other and mixed; Table 1). In this simplified model and compared to Hispanics, subjects' qAF_8 was then predicted by:

$$\log(qAF_8) = 1.221 + 0.732 \cdot \log(age) + 0.079 \cdot white - 0.061 \cdot black - 0.104 \cdot asian + 0.041 \cdot indian \quad (6)$$

The Indian group was made explicit in Equation 6 (although not significantly different from Hispanics) so that all race/ethnicity groups are clearly identified. Equation 6 can be rewritten as:

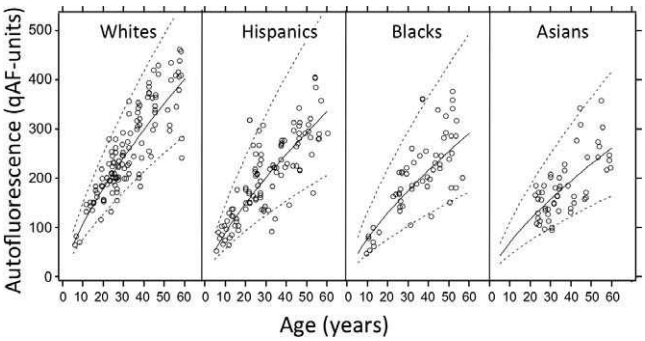

Figure 4. Average qAF (*solid line*) and 95% confidence limits (*dashed lines*) for individuals reporting a single race/ethnicity.

$$qAF_8 = B \cdot age^{0.732} \quad \text{with}$$
$$B = 10^{(1.221 + 0.079 \cdot white - 0.061 \cdot black - 0.104 \cdot asian + 0.041 \cdot indian)} \quad (7)$$

As an example, the prediction for white healthy eyes is:

$$B = 10^{(1.221 + 0.079)} = 19.98, \quad \text{and} \quad qAF = 19.98 \cdot \mathrm{age}^{0.732}$$

and for a 45-year-old Hispanic person, the prediction is:

$$B = 10^{1.221} = 16.64, \quad \text{and}$$
$$qAF = 16.64 \cdot 45^{0.732} = 270\text{qAF-units}$$

The coefficients for *B* and for the 95% confidence limits (calculated from the residuals) for the different race/ethnicity groups separately, and for all groups together are given in Table 2. Mean and confidence limits are illustrated in Figure 4 (the confidence limits are not illustrated for the Indians). Despite having higher qAF on average, the confidence intervals (CIs) for white race were smaller than for the other three race/ethnicities.

For all 277 subjects of the study and for the 262 reporting only one race/ethnicity, lower qAF values were found for subjects with brown irides if the model did not include race/ethnicity identifiers ($P < 0.0001$), but the effect was not significant if those identifiers were included ($P > 0.40$). Among the subjects of white race, when corrected for age, no significant difference in qAF was found between those with blue, green, hazel or brown iris color (Kruskal-Wallis, $P = 0.4$) nor between those with brown and nonbrown iris ($P = 0.30$).

Repeatability

Between-session repeatability of qAF_8 (mean of 2 images/session) was evaluated from images of 233 eyes (179 subjects). The repeatability coefficient for ($\log[qAF_2] - \log[qAF_1]$) was ±0.039 log qAF-units or ±9.4% of the mean qAF_8 ($10^{0.039} - 1 = 0.094$). Repeatability for operator JPG and TD was ±9% and ±12%, respectively. The second session had a slightly higher qAF_8 than the first session (by 1.5%, $P < 0.0001$). This, in part, resulted from a slightly lower ($GL_R - GL_0$) for the internal reference in the second session compared with the first session (by 0.5%, $P < 0.0001$). This effect was observed previously,[30] and may be related to a systematic error in the zero level.

Agreement between operators was evaluated by comparing the qAF_8s obtained in the first session by each operator (38 eyes, 36 subjects). The agreement coefficient was ±0.054 log qAF-units or ±13% of the mean qAF_8. There was no difference in the qAF_8 obtained by the two operators ($P = 0.5$).

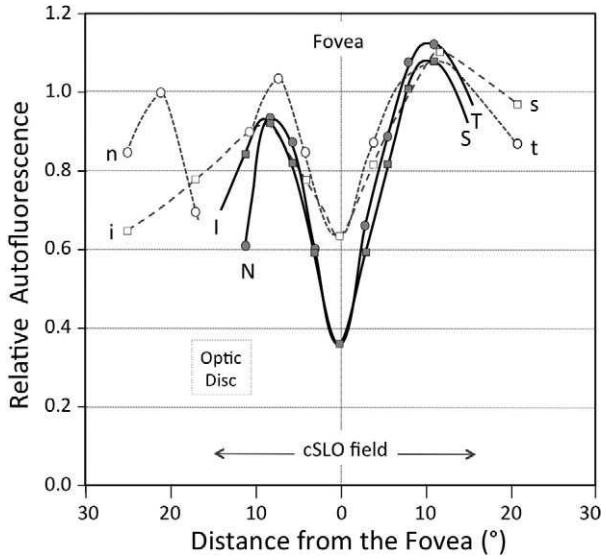

FIGURE 5. Comparison of the spatial distribution of the AF determined in the current study using the SLO (Exc.: 488 nm; *thick lines*, *filled symbols*) and by fluorophotometry (Exc.: 550 nm; *interrupted lines*, *open symbols*) in a previous study.[20] The values are plotted as a function of distance from the fovea along the nasal (N,n) to temporal (T,t) and superior (S,s) to inferior (I,i) axes (linear scale). Data were normalized to the average value at approximately 8.5° from the fovea (center location of the middle ring) (qAF_i/qAF_8). The profiles measured in this study are affected by macular pigment absorption, whereas those measured previously were not. qAF values were determined within a 30° SLO field.

Agreement Between Eyes

The between-eyes coefficient of agreement for 97 subjects was ±0.032 log qAF-units or ±15.3% of the mean qAF_8. As detected by the mixed-effects linear regression, the qAF_8 of right eyes was 0.0072 log qAF-units higher than that of left eyes, corresponding to a 1.7% difference. The right eye was measured first in 75% of the interocular comparisons. The qAF_8 of the second eye was not different from that of the first eye ($P = 0.4$, full model), indicating that the lack of randomization had no influence, even though there was a small (1.5%) difference between two sessions of the same eye.

Discussion

We have compiled and analyzed qAF measurements from a large number of healthy subjects across a broad age range. As expected, qAF values increased monotonically with age. qAF values also varied with race/ethnicity with significantly higher qAF being observed for whites and significantly lower qAF in blacks and Asians as compared with Hispanics. qAF was higher in females as compared with males, but was not related to axial length and smoking status.

Attaining reliable qAF measurements is critically dependent upon good image quality. The operator must be experienced and skilled, and must follow established protocols[30] (also see Methods section). Key requirements for images suitable for qAF measurement are: uniform and maximal signal intensity, fine-tuned focus, central alignment of the camera with the eye to avoid obstruction by the iris, and exposure within the range of linearity of the detector. Technical improvements to aid in the acquisition of suitable images may be the use of a smaller detection aperture to minimize iris obstruction, software driven feedback to warn the operator of less than optimal exposure and uniformity, and ancillary optics to provide a view of the iris during image acquisition. Furthermore, it is important to inspect the acquired video for frames that are partially obscured or of low exposure. Software to identify such frames would be an important addition to the image analysis. Finally, the ability to easily adjust the laser power during image acquisition (the internal reference would compensate for this change) could ease imaging of subjects with photophobia. Reducing the laser power to minimize light exposure for patients with certain retinal degenerations[35] would not substantially reduce total light dose because this would necessitate proportionally longer bleaching duration. Whether a reduced photopic exposure could be achieved using longer excitation wavelengths remains to be investigated.

Spatial Distribution

Nonuniformities in excitation and detection efficiency across the field are the result of both instrumental nonuniformities and nonuniformities resulting from slight misalignment and/or focus. Nonuniformities described here are for the Spectralis used in this study; with other devices the extent of nonuniformity may be different. The issue of nonuniformity is important as it could impact clinical studies of retinal disease if fixation loci are not centered in the field of view. This problem would necessitate increased sample sizes and impact comparisons of data amongst clinical centers.

The spatial distribution of qAF calculated using cSLO images in the current work, (Fig. 5) confirms previous spectrophotometric characterization performed by measuring intensities along the four cardinal meridians.[20] Specifically, both methods determined that AF intensities were greatest superotemporally. Differences in the patterns observed at the fovea are attributable to the use of 550-nm excitation for the spectrophotometric measurements; the latter design ensured that the exciting light was not affected by macular pigment absorption.

Effect of Age

The factor exhibiting the strongest association with qAF was age. Consistent with this, spectrofluorometric measurements (Excitation [Exc.]: 550 nm) of fundus AF in a cohort of healthy subjects aged 20 to 70 years[20] previously revealed that fluorescence intensity increased quasilinearly with age. However, the reflectometry method[36] used in the earlier study was found to overestimate media absorption when the AF was very high, indicating that fundus reflectance may be affected by high amounts of lipofuscin ('vermillion' fundus in Stargardt disease). Thus, here we used normative data for the media transmission (Equation 2).[33] To compare the time course of lipofuscin accumulation predicted by the two sets of data, we recomputed the media correction for the previous data with Equation 2. Multiple regression analysis on both sets of data showed that qAF increased with age$^{0.90}$ and age$^{0.73}$ for the previous and current study, respectively ($P = 0.02$). Thus, the current data reflect an increase in lipofuscin that is slower (Fig. 6). The difference may be explained by changes in the excitation spectrum of fundus AF with age, by imperfection of the algorithm, or by differences in light losses in the ocular media in confocal and notconfocal optical systems. This issue is still under investigation.

These considerations underscore the importance of accounting for light losses in the ocular media; excitations with wavelengths longer than 540 nm would minimize the correction needed and still provide reliable images.[13,14] Taken together however, our findings indicate that after age 20, lipofuscin levels, measured as qAF, undergo a 2-fold increase over a period of 20 to 30 years. In previous studies, fundus AF

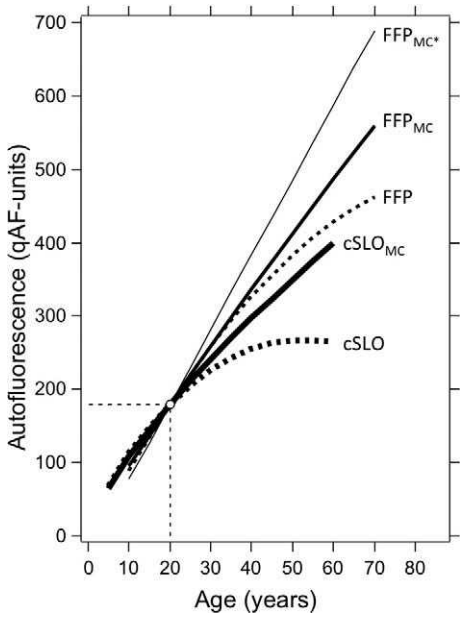

FIGURE 6. Age-related change in AF for data acquired with the cSLO in this study (Exc.: 488 nm) and with the fundus fluorophotometer (FFP) in a previous study (Exc.: 550 nm). The FFP data was normalized to the mean qAF at 20 years of age. The *interrupted curves* are fits through the original data, not accounting for media absorption. High absorption of the 488-nm excitation in older lenses causes the uncorrected cSLO data to decrease for ages older than 55 years. The *continuous lines* are the media corrected (subscript MC) qAF's obtained using the same algorithm (Equation 2) with a coefficient of 5.56×10^{-5} for the 488-nm excitation and 1.33×10^{-5} for 550-nm excitation. The *thin line* (FFP$_{MC*}$) is the FFP data corrected using media absorption derived from a reflectometry method.

also exhibited a propensity to decline after age 70[37]; for this reason and to avoid pronounced age-related changes in ocular media transmission, the upper limit of the age range was restricted to 60 in the current work.

Race/Ethnicity

The observation of racial differences in qAF is consistent with previous morphometric measurements of donor eyes revealing that blacks exhibited approximately 26% less RPE lipofuscin than age-matched whites.[9] This compares with approximately 27% in the present study (Table 2). One cannot reject an, as yet unknown, genetic basis for the differences we observed. Similarly, life-style factors such as nutrition could also make a contribution to these differences. The observation that iris color was not a significant effect when race/ethnicity was accounted for, may reflect the limitations of iris color as an index of pigmentation particularly among dark irides. The exploration of race versus iris melanin concentration may be facilitated by the availability of more sensitive measures of iris stromal pigmentation, such as iris reflectometry.[38]

RPE melanin cannot explain the race/ethnicity-based differences in qAF. RPE cells are derived from neuroepithelium and studies measuring melanin content[39] and light transmission[9] have shown that RPE melanin content is the same for all races[9] and iris color.[39] On the other hand, melanocytes in choroidal and iris stroma are derived embryologically from neural crest and the melanin concentration in these cells varies with the race of the individual. Accordingly, iris color, as documented in this study, is an assessment of pigmentation in both the choroid and iris. Iris color is primarily determined by the amount of melanin in melanocytes of the iris stroma and by absorption/scattering in the superficial iris.[40,41] With respect to qAF, iris and choroidal melanin could affect the AF signal in the images (without lipofuscin change) or could modulate the amount of lipofuscin that accumulates in the RPE. Both of these possibilities are discussed below.

Melanin pigmentation in the choroidal stroma causes fundus reflectance to be higher for subjects with light irides than those with dark irides, particularly in red light. As a result fundus AF would be affected by RPE fluorescence emitted towards the deeper layers and reflected back to augment, particularly in lightly pigment eyes, the RPE fluorescence emitted toward the pupil. Similarly, lipofuscin would also be excited by light reflected by the deeper layers. Using fundus reflectance data from a previous study[20,36] we estimated the magnitudes of these effects (Supplementary Data S3). If the amount of RPE lipofuscin were the same in whites and nonwhites, we found that reflected AF and excitation light would increase the AF signal by at most 6.8% and 4.5% for whites and blacks, respectively. Thus, for an equal amount of lipofuscin, the AF in whites would be 1.068/1.045 or 1.02 times higher than in blacks, much smaller than the ratio qAF(whites)/qAF(blacks) of 1.38 observed in this study (Table 2). Thus, it is unlikely that the effect of reflected emission light plays a significant role in the modulation of qAF by ocular pigmentation.

Melanin pigmentation in the iris has no effect on light adapted pupil diameter[42] but a lightly pigmented eye (blue) allows more light to be transmitted through the iris and through the eye wall posterior to the iris, than does a darkly pigmented brown eye.[43,44] Consequently, subjects having lighter iris pigmentation also have increased intraocular stray light, reduced contrast sensitivity and larger b-wave amplitudes at all illuminance levels.[45,46] Nonetheless, while considerable evidence indicates that RPE lipofuscin formation and the presence of fundus AF depends on a functioning retinoid cycle,[47] whether the extent of lipofuscin accumulation varies with light exposure is unresolved. Also at issue is whether the retinaldehyde isomer driving lipofuscin (e.g., A2E) synthesis is the dark- (11-cis-retinal) or light-induced (all-trans-retinal) form or both. For instance, it was initially reported that in *Abca4*$^{-/-}$ mice, age-related deposition of lipofuscin and in particular A2E was interrupted if the mice were transferred to continuous darkness[48]; however, more recently it was found that A2E accumulated at similar levels in dark-reared and cyclic-light reared mice.[49] It is also notable that bisretinoids of RPE lipofuscin undergo photodegradation[50]; this process would reduce the amount of lipofuscin accumulated. Since many of the photodegradation products are nonfluorescing small molecular fragments,[51,52] qAF would also be decreased.

Other Factors Influencing qAF

We noted other effects that while small, nevertheless, exhibited significant associations (Equation 5). Females had higher qAF (by ~7%) than males. An explanation for this difference is not immediately apparent. The slightly increased qAF_8 in right eyes compared with left eyes appears be due to a 2° to 4° tilt in our Spectralis' table (the tilt was affected by how heavily the subject leaned on the chin rest). Therefore, as accounted for by mirror symmetry, fundi of left eyes were tilted by ≈5° counterclockwise compared with that of right eyes (as observed previously[53]) and the horizontal distance FD (Fig. 1) was greater in right eyes ($P < 0.001$). Accordingly, the middle ring in right eyes was usually positioned at a greater eccentricity and, thus, yielded higher qAF. Detailed analysis based on mean radial qAF gradients predicted that qAF would be $0.7 \pm 1.3\%$ larger in right than left eyes, consistent with the

observed difference of 1.7% (Equation 5). The tendency for qAF to increase with pupil diameter during testing, reflects the fact that with a small pupil (6.5 mm) and eye/head movements, the iris may have partially obstructed the detection aperture (6-mm diameter) of the camera.[30] Since the average pupil diameter after dilation is decreased in older subjects, we have reduced the diameter of the detection aperture of the Spectralis at Columbia University to 5 mm for future studies. Finally, the tendency for qAF to decrease with defocus is not understood but may be related to calibration differences between the focus of the Spectralis and that of the autorefractor.

Considerations With Respect to Intersubject Variability

The between-subject variability in qAF increased with age, similarly to that observed in morphometric measurements[54] and by spectrofluometry.[20] However, variability of log-qAF was ±0.24 log qAF-units (Table 2, all subjects) and did not vary with age. Thus, the between-subject variability in qAF relative to the mean qAF is also not affected by age (±57% of the mean qAF). This proportional increase in the between-subject variability could indicate that the rate of accumulation of lipofuscin (deposition and loss by photodegradation) has been determined at a very young age, presumably mainly by genetic factors (e.g., race, sex). Otherwise, the variability should increase in a nonproportional manner, as people would be affected differently by their environment. While according to this interpretation, the environment may influence lipofuscin accumulation to a lesser extent than genetics, there are several external factors (e.g., antioxidant status, diet, exposure to xenobiotic agents, and/or possibly light exposure) that could play a role during the subjects' lives.

The measurement error characterized by the between-session repeatability was ±0.039 log qAF-units at all ages (95% CIs). Thus, the measurement variability was approximately 6.2 times smaller than the between-subjects variability (0.24/0.039). To illustrate this, we have included in Figure 3 two brackets representing the ±95% CIs of measurement repeatability (approximately ±9% at all ages) at two arbitrary qAF_8 values.

Considerations With Respect to Disease Risk

While the etiology of AMD is complex, there has long been interest in whether RPE lipofuscin contributes to the pathogenesis of this disorder. Several studies have demonstrated that age is the major risk factor for AMD[55]; age is also the principle predictor of qAF. Amongst other demographic variables, female sex has been associated with greater prevalence rates of AMD in some,[56,57] but not all,[58] studies. Thus, we note that qAF was also significantly higher in females. AMD is more frequent in whites than in blacks in the United States; this includes both neovascular AMD and geographic atrophy.[59] Interestingly, in some,[60–64] but not all,[65] case control and cross-sectional studies, fewer AMD cases had brown irides as compared with controls. In another study, severity of choroidal neovascularization was greater in patients with light irides.[66] These studies have been interpreted as indicating that brown iris color is protective against the development of AMD. Nevertheless, the relationship between AMD and race/ethnicity cannot be viewed solely as an effect of ocular pigmentation since amongst the genes known to confer increased susceptibility to AMD, the frequencies of genetic polymorphisms carrying AMD risk vary across race/ethnicities.[59,67] Cigarette smoking is the strongest modifiable risk factor for AMD, and has also been shown to modify the effect of some genetic polymorphisms on AMD risk.[56] However, we found only a tendency for qAF to increase in those who ever smoked. Insufficient power may have been a factor since only 9% of our subjects were smokers and 21% past smokers.

qAF in Future Studies of Retinal Disorders

In clinical settings, interpretations of fundus AF will be facilitated by the ability to ascertain abnormally high or low AF levels in given fundus areas using established normative qAF data together with qAF spatial distribution. qAF will have utility in the diagnosis and monitoring of many retinal disorders. For instance, the bisretinoids of RPE lipofuscin are significantly enhanced in retinal disorders caused by mutations in *ABCA4*, including recessive Stargardt disease, and some forms of cone-rod dystrophy and retinitis pigmentosa.[68–70] Given the pronounced genetic heterogeneity of *ABCA4,* qAF will be vital in establishing genotype–phenotype correlations, and in identifying *ABCA4*-affected patients that are appropriate for clinical trials of small molecule and gene therapies. qAF could also serve to assess the efficacy of these therapeutic interventions. Furthermore, qAF may aid in the differential diagnosis of disorders such as late-onset Stargardt disease versus AMD[71] and in assessing risk for development of AMD. qAF will also assist in resolving whether there is a generalized increase in lipofuscin throughout the retina in Best vitelliform macular dystrophy, which has been an important issue in the field for years.[72–77] In all of these and other disorders, qAF will aid in achieving a better understanding of disease pathogenesis and progression.

Acknowledgments

Supported by grants from the National Eye Institute (R24 EY019861, NEI R01 EY015520), Foundation Fighting Blindness, New York City Community Trust, Roger H. Johnson Fund (University of Washington, Seattle), and a grant from Research to Prevent Blindness to the Department of Ophthalmology, Columbia University.

Disclosure: **J.P. Greenberg**, None; **T. Duncker**, None; **R.L. Woods**, None; **R.T. Smith**, None; **J.R. Sparrow**, None; **F.C. Delori**, None

References

1. Delori FC, Dorey CK, Staurenghi G, Arend O, Goger DG, Weiter JJ. In vivo fluorescence of the ocular fundus exhibits retinal pigment epithelium lipofuscin characteristics. *Invest Ophthalmol Vis Sci*. 1995;36:718–729.
2. Eldred GE. Age pigment structure. *Nature*. 1993;364:396.
3. Parish CA, Hashimoto M, Nakanishi K, Dillon J, Sparrow JR. Isolation and one-step preparation of A2E and iso-A2E, fluorophores from human retinal pigment epithelium. *Proc Natl Acad Sci U S A*. 1998;95:14609–14613.
4. Fishkin N, Sparrow JR, Allikmets R, Nakanishi K. Isolation and characterization of a retinal pigment epithelial cell fluorophore: an all-trans-retinal dimer conjugate. *Proc Natl Acad Sci U S A*. 2005;102:7091–7096.
5. Wu Y, Fishkin NE, Pande A, Pande J, Sparrow JR. Novel lipofuscin bisretinoids prominent in human retina and in a model of recessive Stargardt disease. *J Biol Chem*. 2009;284:20155–20166.
6. Yamamoto K, Yoon KD, Ueda K, Hashimoto M, Sparrow JR. A novel bisretinoid of retina is an adduct on glycerophosphoethanolamine. *Invest Ophthalmol Vis Sci*. 2011;52:9084–9090.
7. Wing GL, Blanchard GC, Weiter JJ. The topography and age relationship of lipofuscin concentration in the retinal pigment epithelium. *Invest Ophthalmol Vis Sci*. 1978;17:601–607.

8. Feeney-Burns L, Hilderbrand ES, Eldridge S. Aging human RPE: morphometric analysis of macular, equatorial, and peripheral cells. *Invest Ophthalmol Vis Sci*. 1984;25:195–200.
9. Weiter JJ, Delori FC, Wing GL, Fitch KA. Retinal pigment epithelial lipofuscin and melanin and choroidal melanin in human eyes. *Invest Ophthalmol Vis Sci*. 1986;27:145–151.
10. Boulton M, Docchio F, Dayhaw-Barker P, Ramponi R, Cubeddu R. Age-related changes in the morphology, absorption and fluorescence of melanosomes and lipofuscin granules of the retinal pigment epithelium. *Vision Res*. 1990;30:1291–1303.
11. Delori FC. Spectrophotometer for noninvasive measurement of intrinsic fluorescence and reflectance of the ocular fundus. *Appl Optics*. 1994;33:7439–7452.
12. Delori FC, Fleckner MR, Goger DG, Weiter JJ, Dorey CK. Autofluorescence distribution associated with drusen in age-related macular degeneration. *Invest Ophthalmol Vis Sci*. 2000;41:496–504.
13. Spaide RF. Autofluorescence imaging with the fundus camera. In: Holz FG, Schmitz-Valckenberg S, Spaide RF, Bird AC, eds. *Atlas of Fundus Autofluorescence Imaging*. Berlin–Heidelberg, Germany: Springer-Verlag; 2007:49–54.
14. Morgan JI, Dubra A, Wolfe R, Merigan WH, Williams DR. In vivo autofluorescence imaging of the human and macaque retinal pigment epithelial cell mosaic. *Invest Ophthalmol Vis Sci*. 2009;50:1350–1359.
15. Webb RH, Hughes GW, Delori FC. Confocal scanning laser ophthalmoscope. *Appl Optics*. 1987;26:1492–1449.
16. von Ruckmann A, Fitzke FW, Bird AC. Distribution of fundus autofluorescence with a scanning laser ophthalmoscope. *Br J Ophthalmol*. 1995;79:407–412.
17. von Ruckmann A, Fitzke FW, Bird AC. Fundus autofluorescence in age-related macular disease imaged with a laser scanning ophthalmoscope. *Invest Ophthalmol Vis Sci*. 1997;38:478–486.
18. Schmitz-Valckenberg S, Holz FG, Fitzke FW. Perspectives in imaging technologies. In: Holz FG, Schmitz-Valckenberg S, Spaide RF, Bird A, eds. *Atlas of Fundus Imaging*. Heidelberg, Germany: Springer-Verlag; 2007;331–338.
19. Lois N, Halfyard A, Bird AC, Fitzke FW. Quantitative evaluation of fundus autofluorescence imaged 'in vivo' in eyes with retinal disease. *Br J Ophthalmol*. 2000;84:741–745.
20. Delori FC, Goger DG, Dorey CK. Age-related accumulation and spatial distribution of lipofuscin in RPE of normal subjects. *Invest Ophthalmol Vis Sci*. 2001;42:1855–1866.
21. Cideciyan AV, Aleman TS, Swider M, et al. Mutations in ABCA4 result in accumulation of lipofuscin before slowing of the retinoid cycle: a reappraisal of the human disease sequence. *Hum Mol Genet*. 2004;13:525–534.
22. Greenstein VC, Duncker T, Holopigian K, et al. Structural and functional changes associated with normal and abnormal fundus autofluorescence in patients with retinitis pigmentosa. *Retina*. 2012;32:349–357.
23. Bindewald A, Schmitz-Valckenberg S, Jorzik JJ, et al. Classification of abnormal fundus autofluorescence patterns in the junctional zone of geographic atrophy in patients with age related macular degeneration. *Br J Ophthalmol*. 2005;89:874–878.
24. Holz FG, Bellman C, Staudt S, Schutt F, Volcker HE. Fundus autofluorescence and development of geographic atrophy in age-related macular degeneration. *Invest Ophthalmol Vis Sci*. 2001;42:1051–1056.
25. Gelman R, Chen R, Blonska A, Barile G, Sparrow JR. Fundus autofluorescence imaging in a patient with rapidly developing scotoma. *Retin Cases Brief Rep*. 2012;6:345–348.
26. Robson AG, Egan CA, Luong VA, Bird AC, Holder GE, Fitzke FW. Comparison of fundus autofluorescence in photopic and scotopic fine-matrix mapping in patients with retinitis pigmentosa and normal visual acuity. *Invest Ophthalmol Vis Sci*. 2004;45:4119–4125.
27. Lois N, Halfyard AS, Bird AC, Holder GE, Fitzke FW. Fundus autofluorescence in Stargardt macular dystrophy-fundus flavimaculatus. *Am J Ophthalmol*. 2004;138:55–63.
28. Preising M. Fundus autofluorescence in Best disease. In: Lois N, Forrester JV, eds. *Fundus Autofluorescence*. Philadelphia, PA: Lippincott Williams and Wilkins; 2009:197–205.
29. Duncker T, Tabacaru MR, Lee W, Tsang SH, Sparrow JR, Greenstein VC. Comparison of near-infrared and short-wavelength autofluorescence in retinitis pigmentosa. *Invest Ophthalmol Vis Sci*. 2013;54:585–591.
30. Delori FC, Greenberg JP, Woods RL, et al. Quantitative measurements of autofluorescence with the scanning laser ophthalmoscope. *Invest Ophthalmol Vis Sci*. 2011;52:9379–9390.
31. ANSI. *American National Standard for Safe Use of Lasers (ANSI 136.1)*. Orlando: The Laser Institute of America; 2007.
32. Delori FC, Webb RH, Sliney DH. Maximum permissible exposures for ocular safety (ANSI 2000), with emphasis on ophthalmic devices. *J Opt Soc Am A Opt Image Sci Vis*. 2007;24:1250–1265.
33. van de Kraats J, van Norren D. Optical density of the aging human ocular media in the visible and the UV. *J Opt Soc Am A Opt Image Sci Vis*. 2007;24:1842–1857.
34. Bland JM, Altman DG. Statistical method for assessing agreement between two methods of clinical measurement. *Lancet*. 1986;1:307–310.
35. Cideciyan AV, Swider M, Aleman TS, Roman MI, Sumaroka A, Schwartz SB. Reduced-illuminance autofluorescence imaging in ABCA4-associated retinal degenerations. *J Opt Soc Am A Opt Image Sci Vis*. 2007;24:1457–1467.
36. Delori FC, Burns SA. Fundus reflectance and the measurement of crystalline lens density. *J Opt Soc Am A Opt Image Sci Vis*. 1995;13:15–26.
37. Delori FC. RPE lipofuscin in ageing and age-related macular degeneration. In: Coscas G, Piccolino FC, eds. *Retinal Pigment Epithelium and Macular Disease (Documenta Ophthalmologica)*. Dordrecht, The Netherlands: Kluwer Academic Publishers; 1995:37–45.
38. Baranoski GVG, Lam MWY. Qualitative assessment of undetectable melanin distribution in lightly pigmented irides. *J Biomed Opt*. 2007;12:030501.
39. Schmidt SY, Peisch RD. Melanin concentration in normal human retinal pigment epithelium. *Invest Ophthalmol Vis Sci*. 1986;27:1063–1067.
40. Imesch PD, Bindley CD, Khademian Z, et al. Melanocytes and iris color. Electron microscopic findings. *Arch Ophthalmol*. 1996;114:443–447.
41. Wielgus AR, Sarna T. Melanin in human irides of different color and age of donors. *Pigment Cell Res*. 2005;18:454–464.
42. Winn B, Whitaker D, Elliott DB, Phillips NJ. Factors affecting light-adapted pupil size in normal human subjects. *Invest Ophthalmol Vis Sci*. 1994;35:1132–1137.
43. van den Berg TJTP, IJspeert JK, deWaard PWT. Dependence of intraocular straylight on pigmentation and light transmission through the ocular wall. *Vision Res*. 1991;31:1361–1367.
44. Coppens JE, Franssen L, van den Berg TJ. Wavelength dependence of intraocular straylight. *Exp Eye Res*. 2006;82:688–692.
45. Wali N, Leguire LE. Fundus pigmentation and the dark-adapted electroretinogram. *Doc Ophthalmol*. 1992;80:1–11.
46. Nischler C, Michael R, Wintersteller C, et al. Iris color and visual functions. *Graefes Arch Clin Exp Ophthalmol*. 2013;25:195–202.

Investigative Ophthalmology & Visual Science

47. Lorenz B, Wabbels B, Wegscheider E, Hamel CP, Drexler W, Presing MN. Lack of fundus autofluorescence to 488 nanometers from childhood on in patients with early-onset severe retinal dystrophy associated with mutations in RPE65. *Ophthalmology*. 2004;111:1585–1594.
48. Mata NL, Weng J, Travis GH. Biosynthesis of a major lipofuscin fluorophore in mice and humans with ABCR-mediated retinal and macular degeneration. *Proc Natl Acad Sci U S A*. 2000;97:7154–7159.
49. Boyer NP, Higbee D, Currin MB, et al. Lipofuscin and N-retinylidene-N-retinylethanolamine (A2E) accumulate in the retinal pigment epithelium in the absence of light exposure: their origin is 11-cis retinal. *J Biol Chem*. 2012;287:22276–22286.
50. Sparrow JR, Gregory-Roberts E, Yamamoto K, et al. The bisretinoids of retinal pigment epithelium. *Prog Retin Eye Res*. 2012;31:121–135.
51. Wu Y, Yanase E, Feng X, Siegel MM, Sparrow JR. Structural characterization of bisretinoid A2E photocleavage products and implications for age-related macular degeneration. *Proc Natl Acad Sci U S A*. 2010;107:7275–7280.
52. Yoon KD, Yamamoto K, Ueda K, Zhou J, Sparrow JR. A novel source of methylglyoxal and glyoxal in retina: implications for age-related macular degeneration. *PLoS One*. 2012;7:e41309.
53. Duncker T, Greenberg JP, Sparrow JR, Smith RT, Quigley HA, Delori FC. Visualization of the optic fissure in short-wavelength autofluorescence images of the fundus. *Invest Ophthalmol Vis Sci*. 2012;53:6682–6686.
54. Okubo A, Rosa RHJ, Bunce CV, et al. The relationships of age changes in retinal pigment epithelium and Bruch's membrane. *Invest Ophthalmol Vis Sci*. 1999;40:443–449.
55. Age-Related Eye Disease Study Research Group. Risk factors associated with age-related macular degeneration. A case-control study in the age-related eye disease study: Age-Related Eye Disease Study Report Number 3. *Ophthalmology*. 2000;107:2224–2232.
56. Naj AC, Scott WK, Courtenay MD, et al. Genetic factors in nonsmokers with age-related macular degeneration revealed through genome-wide gene-environment interaction analysis. *Ann Hum Genet*. 2013;77:215–231.
57. Rudnicka AR, Jarrar Z, Wormald R, Cook DG, Fletcher A, Owen CG. Age and gender variations in age-related macular degeneration prevalence in populations of European ancestry: a meta-analysis. *Ophthalmology*. 2012;119:571–580.
58. Klein R, Myers CE, Meuer SM, et al. Risk alleles in CFH and ARMS2 and the long-term natural history of age-related macular degeneration: the Beaver Dam Eye Study. *JAMA Ophthalmol*. 2013;131:383–392.
59. Klein R. Race/ethnicity and age-related macular degeneration. *Am J Ophthalmol*. 2011;152:153–154.
60. Hyman LG, Lilienfeld AM, Ferris FL, Fine SL. Senile macular degeneration: a case-control study. *Am J Epidemiol*. 1983;118:213–227.
61. Holz FG, Piguet B, Minassian DC, Bird AC, Weale RA. Decreasing stromal iris pigmentation as a risk factor for age-related macular degeneration. *Am J Ophthalmol*. 1994;117:19–23.
62. Weiter JJ, Delori FC, Wing GL, Fitch KA. Relationship of senile macular degeneration to ocular pigmentation. *Am J Ophthalmol*. 1985;99:185–187.
63. Frank RN, Pukin JE, Stock C, Canter LA. Race, iris color, and age-related macular degeneration. *Trans Am Ophthalmol Soc*. 2000;98:109–117.
64. Chakravarthy U, Wong TY, Fletcher A, et al. Clinical risk factors for age-related macular degeneration: a systematic review and meta-analysis. *BMC Ophthalmol*. 2010;10:31.
65. Vinding T. Pigmentation of the eye and hair in relation to age-related macular degeneration. An epidemiological study of 1000 aged individuals. *Acta Ophthalmol*. 1990;68:53–58.
66. Sandberg MA, Gaudio AR, Miller S, Weiner A. Iris pigmentation and extent of disease in patients with neovascular age-related macular degeneration. *Invest Ophthalmol Vis Sci*. 1994;35:2734–2740.
67. Spencer KL, Glenn K, Brown-Gentry K, Haines JL, Crawford DC. Population differences in genetic risk for age-related macular degeneration and implications for genetic testing. *Arch Ophthalmol*. 2912;130:116–117.
68. Martinez-Mir A, Paloma E, Allikmets R, et al. Retinitis pigmentosa caused by a homozygous mutation in the Stargardt disease gene ABCR. *Nat Genet*. 1998;18:11–12.
69. Shroyer NF, Lewis RA, Allikmets R, et al. The rod photoreceptor ATP-binding cassette transporter gene, ABCR, and retinal disease: from monogenic to multifactorial. *Vision Res*. 1999;39:2537–2544.
70. Eagle RC, Lucier AC, Bernardino VB, Yanoff M. Retinal pigment epithelial abnormalities in fundus flavimaculatus. *Ophthalmology*. 1980;87:1189–1200.
71. Westeneng-van Haaften SC, Boon CJ, Cremers FP, Hoefsloot LH, den Hollander AI, Hoyng CB. Clinical and genetic characteristics of late-onset Stargardt's disease. *Ophthalmology*. 2012;119:1199–1210.
72. Frangieh GT, Green R, Fine SL. A histopatholgic study of Best's macular dystrophy. *Arch Ophthalmol*. 1982;100:1115–1121.
73. Bakall B, Radu RA, Stanton JB, et al. Enhanced accumulation of A2E in individuals homozygous or heterozygous for mutations in BEST1 (VMD2). *Exp Eye Res*. 2007;85:34–43.
74. Weingeist TA, Kobrin JL, Watzke RC. Histopathology of Best's macular dystrophy. *Arch Ophthalmol*. 1982;100:1108–1114.
75. O'Gorman S, Flaherty WA, Fishman GA, Berson EL. Histopathological findings in Best's vitelliform macular dystrophy. *Arch Ophthalmol*. 1988;106:1261–1268.
76. Spaide RF, Noble K, Morgan A, Freund KB. Vitelliform macular dystrophy. *Ophthalmology*. 2006;113:1392–1400.
77. Mullins RF, Kuehn MH, Faidley EA, Syed NS, Stone EM. Differential macular and peripheral expression of bestrophin in human eyes and its implication for Best disease. *Invest Ophthalmol Vis Sci*. 2007;48:3372–3380.

Investigative Ophthalmology & Visual Science